J Mater Sci (2007) 42:7586–7591
DOI 10.1007/s10853-007-1879-0

Rolling and recrystallisation textures in Cu–Al, Cu–Mn and Cu–Ni alloys

Subramanya Sarma Vadlamani · Joerg Eickemeyer · Ludwig Schultz · Bernhard Holzapfel

Received: 27 September 2005 / Accepted: 25 May 2006 / Published online: 23 June 2007

Abstract The development of strongly cube textured Cu based substrates is important in the cost effective production of long lengths of high temperature superconducting cables. The present paper reports textures (deformation and recrystallisation) development in pure Cu, Cu–Al, Cu–Mn (with a solute content of 1–3 at.%) and Cu–35 at.% Ni alloys.

Introduction

Significant progress has been made in the development of long lengths of second-generation high temperature superconducting (HTS) wires using the Rolling Assisted Biaxially Textured Substrates (RABiTS^{TM}) process [1]. In this method, the desired strong biaxial texture in the superconducting YBCO film is achieved by epitaxial growth of a buffer and YBCO film on a highly textured thin metallic substrate. To date, many reports have been published on coated conductors manufactured using the RABiTS technique where YBCO is deposited on cube textured Ni or Ni alloy substrates, with intervening buffer layers for chemical separation and improved lattice matching [2–6]. However, the YBCO coated conductors are still underdeveloped in terms of AC losses, low cost, enhanced stability and quench protection. Alternative Cu-based coated conductors have thus been proposed where textured Cu is used as the substrate [7, 8]. Copper based substrates have the advantages of easy formation of a sharp cube texture, no ferromagnetic contribution to hysteretic AC losses, low cost compared to Ni or Ni alloy substrates and low resistivity. However, Cu has very low mechanical strength and poor oxidation resistance in comparison to Ni and Ni alloys. Development of high strength Cu alloys with strong recrystallisation cube texture is therefore very important in the economical production of coated conductors. The present investigation is aimed at the development of strongly cube textured copper alloys with improved strength.

S. S. Vadlamani (✉)
Department of Metallurgical and Materials Engineering, Indian Institute of Technology Madras, Chennai 600 036, India
e-mail: vsarma@iitm.ac.in

J. Eickemeyer · L. Schultz · B. Holzapfel
Institute for Solid State and Materials Research (IFW), Helmholtz strasse 20, Dresden 01069, Germany

Selection of alloys

For improving the mechanical properties, alloying with elements (which can dissolve and form substitutional solid solutions) is the only strengthening mechanism possible. It is well established that the recrystallisation cube texture is strongly related to the rolling texture [9]. A metal (copper) type rolling texture characteristic of high stacking fault energy (SFE) metals/alloys promotes recrystallisation cube texture while alloy (brass) rolling texture characteristic of low SFE metals/alloys was shown to promote recrystallisation twinning [10, 11]. Available data on SFE of Cu alloys shows that except for Mn and Ni, all other alloying additions (Al, Ge, Zn) lead to sharp drop in SFE [12, 13]. The variation of SFE with solute concentration of Mn and Al (taken from Ref. [13] is given in Fig. 1. It has also been reported that addition of ≥4 at.% Mn resulted in a sharply reduced cube texture [14]. Based on the above available information in the literature, we have selected Cu–Al, Cu–Mn and Cu–Ni alloys for investigation. It may be noted

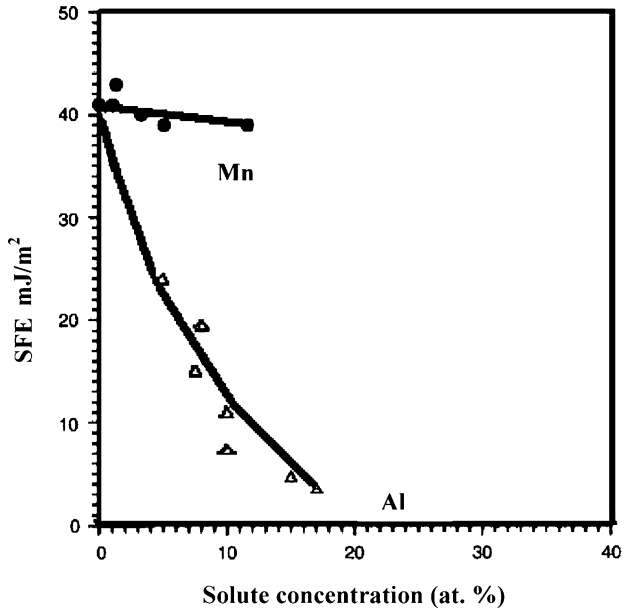

Fig. 1 Variation of Stacking Fault Energy (SFE) of Cu–Al and Cu–Mn alloys (from ref. [13])

that Cu–Ni alloys have complete solid solubility throughout the compositional regime. However, addition of ~38 at.% of Ni to Cu results in increase in Curie temperature to >77 K. Therefore Cu–35 at.% Ni alloy which has Cuie temperature <77 K was selected for investigation. The present paper discusses the rolling and recrystallisation texture development in Cu, Cu–Al, Cu–Mn (in the range of 1–3 at.% alloying addition) and Cu–35 at.% Ni alloys.

Experimental

Cu, Cu–Al, Cu–Mn (with solute concentrations of 1, 2 and 3 at.%) and Cu–35 at.% Ni alloys were prepared from elements with purities of 99.98% in an induction furnace and casting (in argon atmosphere) them to 15 × 15 mm size. The ingots were hot rolled to 10 × 10 mm^2 followed by cold rolling (10% reduction per pass) to 2 mm thickness. At this stage, an intermediate recrystallisation annealing (400–600 °C for 30 min depending on alloy content) was done to develop a fine grain size. The annealed strips were further cold rolled in several passes (10% reduction per pass) to substrates of 80 μm thickness (96% total thickness reduction) and 10 mm width. For X-ray texture analysis {111}, {200}, {220} and {311} pole figures were measured in steps of 3° between 0 and 70° on a Philips X-ray texture goniometer using Cu-Kα radiation. From the incomplete pole figure data, orientation distribution function (ODF) calculations and quantitative texture components analysis (with an angular range of 15°) was performed using commercial texture analysis software LABOTEX [15, 16]. Small strips from all the alloys were recrystallised at 800 °C for 30 min. in Argon +5% H_2 atmosphere. Recrystallisation textures were investigated with electron backscatter diffraction (EBSD) technique using the Channel 5 software of HKL Technolgies, Denmark in the LEO Field Emission Gun Scanning Electron Microscope (FEGSEM) operating at 20 kV. The hardness was measured using a Shimadzu Vickers microhardness tester (HMV 2000) with a 10 g (98 mN) load.

Results

The intermediate annealing at 2 mm resulted in equiaxed grain structure with a mean grain size of 7–10 μm in all the different alloys.

Rolling textures

The variation in volume fraction of important rolling texture components (Copper (Cu) {112}⟨111⟩, S {123}⟨634⟩ and Brass (Bs) {011} ⟨112⟩) with alloy content is shown in Fig. 2. In case of Cu–35% Ni alloy, the Cu, S and Bs components are 12, 40 and 23% respectively. The variation in volume fraction of minor texture components (Goss {110} ⟨001⟩ and Twin of Copper (TC) {552} ⟨115⟩) is given in Table 1. The rolling textures of Cu-Mn and Cu-Al alloys are very similar. The volume fractions of Cu and S orientations progressively decrease and that of Bs orientation increases with increasing Al and Mn alloy content

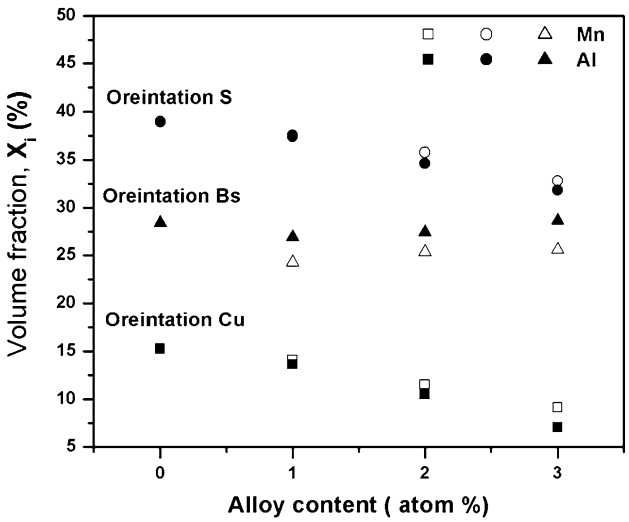

Fig. 2 Variation of Copper, S and Brass texture components with alloy content

Table 1 Volume fractions of Goss and Twin of Cu (TC) orientations as a function of alloy content

Alloy	Goss (%)	TC (%)
Cu	0	0
Cu–1% Mn	6.5	5.7
Cu–2% Mn	7.9	7.4
Cu–3% Mn	10.1	8.5
Cu–1% Al	6.0	4.6
Cu–2% Al	8	6.9
Cu–3% Al	9.8	7.9
Cu–35% Ni	2	0

(Fig. 2). Also G and TC orientations appear at 1% of Al and Mn and increase slightly with increasing alloy content (Table 1).

Recrystallisation textures

The EBSD maps for the recrystallised pure Cu, Cu–1% Al, Cu–1% Mn and Cu–35% Ni are shown in Fig. 3a–d respectively. The (111) pole figures for the recrystallised pure Cu, Cu–1% Al and Cu–1% Mn alloys are given in Fig. 4a–c respectively. From the EBSD data, the volume fraction of cube texture (within 15° from the ideal cube orientation) is calculated and the variation of cube texture fraction with alloy content is plotted in Fig. 5. For the Cu–35% Ni alloy, the cube texture volume fraction is ~90%. From the EBSD data, the grain sizes and grain boundary character is also determined and these data are given in Table 2.

From Figs. 3, 4 and 5 it can be seen that very strong cube texture is developed in pure Cu and the cube fraction decreases drastically with additions of Al and Mn. The decrease is much more steep in case of Cu–Al alloy in comparison to Cu–Mn alloy. From the pole figures (Fig. 4a–c), it can be seen that the in case of Cu–Al alloy, the recrystallisation texture is similar to the deformation texture (Fig. 4b), while recrystallisation twins are major texture component (apart from cube texture) in case of Cu–Mn alloy (Fig. 4c). The recrystallisation texture in the Cu–35% Ni alloy consists of predominantly cube texture and twins of the cube (Fig. 3d). The average grain sizes in the Cu–Al alloys are significantly smaller (10 μm) in comparison to Cu–Mn alloys (35 μm) (see Fig. 3 and Table 2) and Cu–35% Ni alloy (27 μm). The fraction of twin boundaries is found to increase with alloy content in Cu–Mn alloys while there is no clear trend in case of Cu–Al alloys (Table 2).

Hardness

The hardness of the recrystallised alloys is shown in Fig. 6. It is clear that small alloying additions do not contribute much hardening in both Cu–Al and Cu–Mn alloys though the hardness increase in Cu–Mn is slightly higher in comparison to Cu–Al system. The hardness for the Cu–35% Ni alloy is around 120 HV in the recrystallised condition.

Discussion

Texture transition from Cu to Bs type in the rolling texture has been reported with increasing alloying content in many Cu alloys [10, 13, 17], Ni–Co, Ni–Cr and Ni–W alloys [18–20]. This is usually attributed to the lowering of stacking fault energy (SFE) or the suppression of cross slip with increasing alloying content which in turn promotes twinning and shear banding [10, 21].

Hirsch et al. [10] proposed the following mechanism for the texture transition in medium SFE materials: (1) twinning of the Cu {112} ⟨111⟩ leading to TC {552} ⟨115⟩ in the form of few isolated twins, (2) slip on TC on the two systems with highest resolved shear stress leading to rotation of TC around ⟨110⟩ parallel to TD in directions of larger ϕ towards G and (3) slip in G on only two of the four equally preferred systems leading to a rotation around ⟨110⟩ parallel to ND towards Bs. The appearance of G and TC orientations in Cu–Al and Cu–Mn alloys (Table 1) does indeed support the above texture transition mechanism. The above mechanism could be applicable for Cu–Al alloys as SFE in these alloys has been shown to decrease sharply even at small concentrations (Fig. 1). However, in case of Cu–Mn alloys, the SFE is not lowered in the range of alloying addition up to 12 at.% (Fig. 1). Engler [13] has studied deformation textures in Cu–Mn alloys (alloy concentrations of 4–16 at.%) and suggested that short range ordering and increased strength could be responsible for the observed texture transition. However, in the present case, the hardness increase is found to be marginal (135 HV for pure Cu and 141 HV for Cu–1 at.% Mn alloy in the as rolled conditions). It is clear that even small additions of Mn do alter the deformation mechanisms, though the exact mechanisms are not clear and require detailed investigation.

It has been well established that the recrystallisation texture is strongly related to the deformation texture. The strong recrystallisation cube texture in pure Cu is usually attributed to its 40° ⟨111⟩ -orientation relationship with the S orientation in the rolling texture. It must be noted that though the deformation textures in Cu–1 at% Al and Cu–1 at.% Mn are similar, the recrystallisation textures are

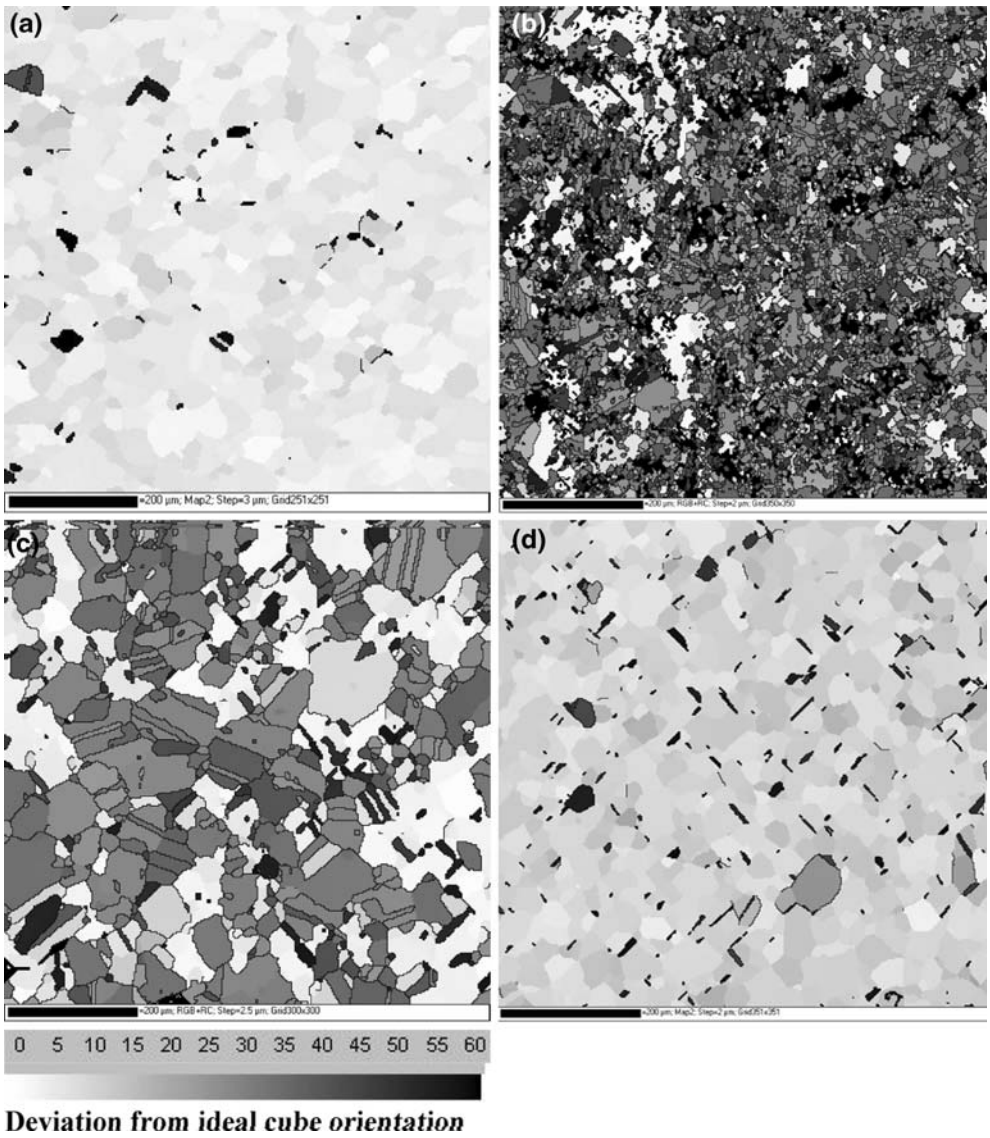

Fig. 3 EBSD maps for recrystallised (**a**) Cu, (**b**) Cu–1 at.% Al, (**c**) Cu–1 at.% Mn and Cu–35% Ni alloys. Grain boundaries above 15 are indicated by black lines

significantly different (Figs. 3–5). The recrystallisation texture in Cu–Al alloys is similar to the deformation texture (Fig. 4b). The recrystallised orientation which is similar to the rolling texture component S (denoted by miller indices {123} ⟨634⟩) is known as R orientation (with the same miller indices as S) in the literature and has been observed in Al alloys [22, 23], in Cu–Ge, Cu–Zn and Cu–P alloys [24–26]. The R orientation has been shown to nucleate from the deformed grains in the vicinity of grain boundaries. If these nuclei reach the grain boundaries, they encounter a mobile high angle grain boundary and hence, they can expand into the neighbouring grain. Owing to their formation in the deformed matrix, such nuclei exhibit orientations close to the rolling texture. The R orientation prevails in Cu-alloys, where the favoured growth of cube oriented grain is retarded by the solutes, but shear band formation and recrystallisation twinning are not yet sufficiently favoured so as to initiate additional nucleation events. It should be noted that recrystallisation twins were also observed in Cu–Al alloys. The recrystallisation cube texture in Cu–Mn alloys is predominantly cube and twin of the cube (Figs. 3–5). The twin boundary fraction has also been found to increase with increasing Mn content within the present experimental range of 1–3 at.% (Table 2). This result however, in contradiction to the findings of Engler [14], where recrystallised twins were reported to be not present in the range of 4–16 at.% Mn alloy content. Recrystallisation twins are believed to be due to growth accidents on propagating {111} steps, which are associated with migrating grain boundary [11]. Higher mobility of the migrating boundary and lower SFE were shown to promote twin boundary formation [11]. Since SFE is not lowered in Cu–Mn alloys, it is possible that the addition of Mn atom increased grain boundary mobility. It is well known that

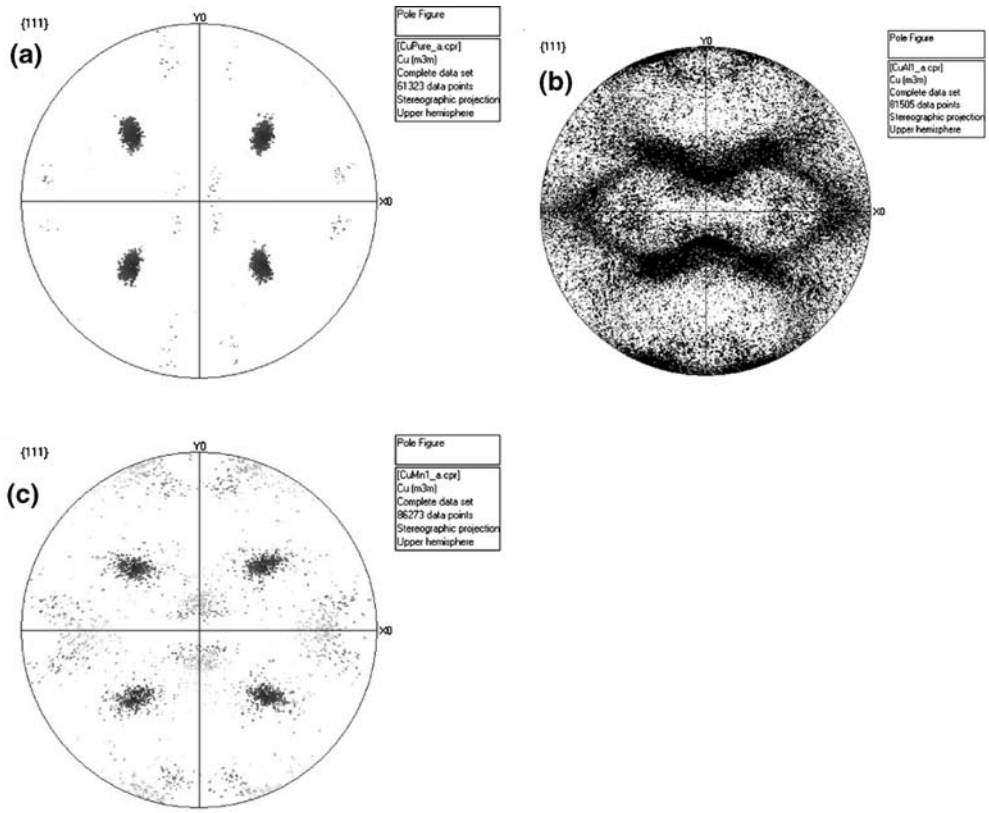

Fig. 4 {111} pole figures (calculated from EBSD data) for recrystallised (**a**) pure Cu, (**b**) Cu–1% Al and (**c**) Cu–1% Mn alloys

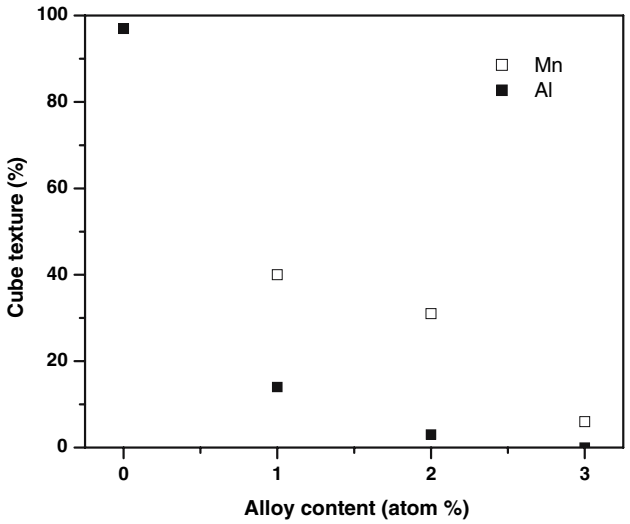

Fig. 5 Cube texture fraction as a function of alloy content in Cu–Al and Cu–Mn alloys

the presence of solute atoms influences the kinetics of grain boundary migration. It is generally believed that larger atoms (bigger atomic radius) retard the diffusion leading to slowing down of grain boundary mobility, which controls the recrystallisation and grain growth kinetics. This effect of solute atoms can be seen from the recrystallisation grain size measurements on Cu–Al, Cu–Mn and Cu–Ni alloys

Table 2 Grain sizes and fraction of $\Sigma 3$ (twin) grain boundaries in different alloys

Alloy	Grain size (μm)	Fraction of $\Sigma 3$ (twin) grain boundaries (%)
Cu	45 ± 37	2
Cu–1% Mn	34 ± 27	27
Cu–2% Mn	30 ± 25	48
Cu–3% Mn	35 ± 30	53
Cu–1% Al	10 ± 9	27
Cu–2% Al	10 ± 10	34
Cu–3% Al	8 ± 11	25
Cu–35% Ni	28 ± 23	11

(Table 2). The recrystallised grain sizes for Cu–Al alloys are significantly smaller (around 10 μm) in comparison to Cu–Mn (35 μm) and Cu–Ni alloys (27 μm). For an assessment of alloying elements in solid solution, (in particular if the elements have different crystal structures) an effective volume size factor has been used [14]. Based on the data in literature (see Table 3 in ref [14]), the Cu–Mn alloys have a effective volume size factor of +34%, Cu–Al alloys +20% and Cu–Ni alloys –8.5%. It is clear that the present experimental results cannot be explained on the basis of the volume size factor also. Further work is necessary to understand the above results.

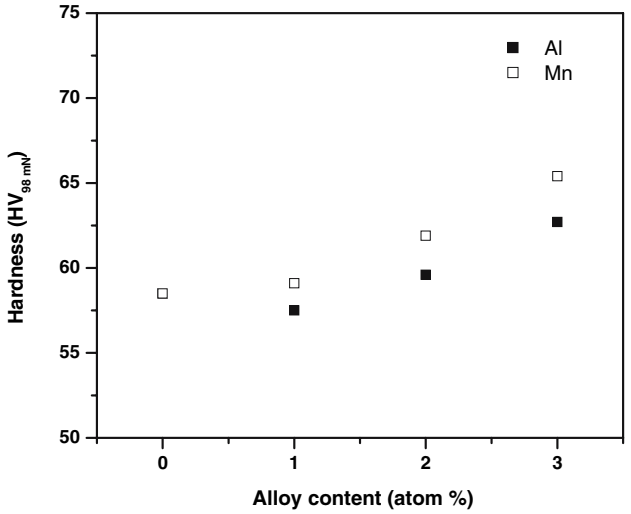

Fig. 6 Hardness as a function of alloy content for Cu–Al and Cu–Mn alloys

Cu–35 at.% Ni has shown the highest cube fraction (~90%) among the alloys considered and hardness is twice that of pure copper. Further improvements in texture strength (to reach >97% cube volume fraction) are necessary for use as RABiTS substrate.

Conclusions

From the investigation of deformation and recrystallisation textures in Cu, Cu–Al, Cu–Mn and Cu–Ni alloys, the following conclusions are arrived at:

(1) The volume fractions of rolling texture components Cu $(112)\langle 111\rangle$ and S $(123)\langle 634\rangle$ decreased and the Brass component (011) $\langle 112\rangle$) increased with increasing Al and Mn content. Goss (110) $\langle 001\rangle$ and Twin of Copper (TC) (552) $\langle 115\rangle$ orientations are present after 1% of Mn/Al additions. The rolling texture of Cu–35% Ni is essentially similar to that of pure Cu.

(2) The recrystallisation Cube (001) $\langle 100\rangle$ texture component (which is the predominant texture component in pure Cu) decreases drastically with increasing Al/Mn additions. On the other hand, Cu–35% Ni alloy exhibited strong cube texture (90%) and could be considered for further research to optimise the texture for application as a substrate material for RABiTS process.

Acknowledgments One of the authors (VSS) gratefully acknowledges the financial support of Alexander von Humboldt Foundation, Bonn, Germany through a research fellowship during which period the above work was completed.

References

1. Norton DP, Goyal A, Budai JD, Christen DK, Kroeger DM, Specht ED, He Q, Saffian B, Paranthaman M, Klabunde CE, Lee DF, Sales BC, List FA (1996) Science 274:755
2. Eickemeyer J, Selbmann D, Opitz R, de Boer B, Holzapfel B, Schultz L, Miller U (2001) Supercond Sci Technol 14:152
3. Eickemeyer J, Selbmann D, Opitz R, Wendrock H, Maher E, Miller U, Prusseit W (2002) Physica C 372–376:814
4. Varesi E, Celentano G, Petrisor T, Boffa V, Ciontea L, Galluzzi V, Gambardella U, Mancini A, Rufuloni A, Vannozzi A (2003) Supercond Sci Technol 16:498
5. Zhou YX, Naguib R, Fang H, Salama K (2004) Supercond Sci Technol 17:947
6. Bindi M, Botarelli A, Gauzzi A, Gianni L, Ginocchio S, Holzapfel B, Baldini A, Zannella S (2004) Supercond Sci Technol 17:512
7. Diaz J, Segarra M, Espiell F, Pinol S (2001) Supercond Sci Technol 14:576
8. Yust NA, Nekkanti R, Brunke LB, Srinivasan R, Srinivasan PN (2005) Supercond Sci Technol 18:9–13
9. Humphreys FJ, Hatherly M (1995) Recrystallisation and related annealing phenomena. Pergamon, Oxford
10. Hirsch J, Lücke K (1988) Acta Metall 36:2883
11. Mahajan S, Pande CS, Imam A, Rath BB (1997) Acta Mater 45:2633
12. Gallagher PCJ (1970) Met Trans A 1:2429
13. Engler O (2000) Acta Mater 48:4827
14. Engler O (2001) Acta Mater 48:1237
15. http://www.labotex.com/
16. Pawlik K (1986) Phys Stat Sol (b) 134:477
17. Hirsch J, Lücke K, Hatherly M (1988) Acta Metall 36:2905
18. Ray RK (1995) Acta Metall Mater 43:3861
19. de Boer B, Reger N, Holzapfel B, Gottstein G, Moldov DA (eds) (2001) First joint international conference on recrystallisation and grain growth. Springer-Verlag, Berlin Heidelberg, pp 1355–1360
20. Subramanya Sarma V, Eickemeyer J, Mickel C, Schultz L, Holzapfel B (2004) Mater Sci Eng A 380:30
21. Leffers T, Pedersen OB (2002) Scripta Mater 46:741
22. Engler O, Vatne HE, Nes E (1996) Mater Sci Eng A 205:187
23. Engler O (1999) Metall Mater Trans 30A:1517
24. Schmidt U, Luecke K (1979) Texture Crystalline Solids 3:85
25. Hutchinson WB, Ray RK (1979) Metal Sci 13:125
26. Eichelkraut H, Hirsch J, Luecke K (1984) Z Metallkd 75:113